Modeling and control of doubly fed induction generator with a disturbance observer: A stator voltage oriented approach

E.Emre ÖZSOY [(1)], Edin GOLUBOVIC [(2)], Asıf ŞABANOVIC [(3)],
Seta BOGOSYAN [(4)], Metin GÖKAŞAN [(5)],
[(1,4,5)] *Istanbul Technical University, Istanbul, Turkey*
[(1,4)] *{eozsoy,gokasan}@itu.edu.tr,* [(3)] *sbogosyan@alaska.edu*
[(2,3)] *Sabancı University, Istanbul, Turkey,*
{edin,asif}@sabanciuniv.edu

Abstract—The popularity of renewable energy conversion systems, especially wind energy has been increasing in recent years. Doubly fed induction generator (DFIG) based wind energy systems are intensively used due to their wide range of active and reactive power controllability. Conventional DFIG control structures consist of decoupled PI rotor current controllers with stator flux orientation and machine parameter dependent compensating terms. The accuracy of stator flux calculation is dependent on how accurately the stator resistance is known. Integration problems also exist and additional low pass filters are implemented to accurately calculate the stator flux. In this study, machine dependent compensating terms are estimated with a first order low pass filter disturbance observer. Therefore, a single proportional (P) controller is sufficient to control decoupled rotor currents. The proposed controller structure is implemented on a Matlab/Simulink platform with the parameters of 500KW DFIG used in MILRES (Turkish National Wind Energy) project. The proposed controller is also experimentally validated in an experimental setup.

Keywords; *Doubly fed induction generator, disturbance observer, wind energy*

Symbol Nomenclature

i_{sa}, i_{sb}, i_{sc} : Stator a, b and c phase currents i_{sd}, i_{sq} : Stator d and q axis currents

i_{ra}, i_{rb}, i_{rc} : Rotor a, b and c phase currents i_{rd}, i_{rq} : Rotor d and q axis currents

v_{sa}, v_{sb}, v_{sc} : Stator a, b and c phase voltages

v_{ra}, v_{rb}, v_{rc} : Rotor a, b and c phase voltages

v_{rd}, v_{rq} : Rotor d and q axis voltages

P_s, : Stator Active Power

L_s, L_r : Stator and rotor inductances

L_{rb} : Base value of rotor inductance

p : Number of pole pairs

ω_m : Rotor mechanical speed

T_e : Electrical Torque

θ_s : Stator electrical angle

T_s : Sample Time

k_p, k_q : Proportional gain of controller

$v_{s\alpha}$, $v_{s\beta}$: α and β axis stator voltage

v_{sd}, v_{sq} : Stator d and q axis voltages

R_s, R_r : Stator and rotor resistances

Q_s : Stator reactive Power

L_m : Mutual inductance

ΔL_r : Disturbance of L_r

ω_s : Stator electrical speed

T_m : Mechanical Torque

b : Viscous friction constant

θ_r : Rotor electrical angle

s : Laplace operator

1. Introduction

Research on renewable energy conversion systems is of great importance due to the rapid consumption of fuel resources and environmental issues. Wind energy conversion systems appear to be the fastest growing technology and most of the electrical energy generated by renewable sources is from wind energy conversion systems [1]. DFIG based wind turbines have important advantages compared to other wind energy conversion systems. For example, 30% of rated stator power is sufficient for the rotor side inverter circuit to achieve 4-quadrant stator active and reactive power flow with a speed variation around ±25%. This reduces the cost and complexity of the overall system.

Considerable research studies are encountered about DFIG modeling and control in the literature. DFIG dynamic equations are fully written in [1, 2]. A complete simulation and modeling for high power DFIG wind farms are given in [3]. Reduced order DFIG dynamic model was also proposed in this study due to simulation constraints.

From orientation frame point of view, basically, stator flux [4] and stator voltage orientation [5] can be encountered in which the position of the stator-flux or voltage space vector is aligned with the d-axis of the d-q frame. Stator flux orientation control techniques are dependent on the accuracy of stator resistance information. Integration problems also exist and additional low pass filters are implemented to accurately calculate stator flux [4]. The effect of stator resistance value can be neglected in flux calculation and stator voltage orientation could be applied by adding 90^{o} phase shift to voltage angle. This may cause additional coupling effect in active and reactive power control, which can be compensated by implementing additional controllers in the outer loop as given in [5]. It is claimed in [6] that controller performances of both orientation frames are equivalent.

The idea of stator voltage orientation with disturbance observer starts with [7]. The scheme of [7] consists of simulation results of direct stator active and reactive power control with disturbance observer.

Synchronization is also another issue to smoothly connect DFIG to the grid. Grid and generated stator voltages must be collinear, which means that equal in phase and amplitude, before DFIG is connected to the grid to prevent high currents. Majority of

the contributions focus on a mode of operation that DFIG is already connected to the grid. Synchronization procedure is comprehensively analyzed in [8] with important citations.

There are also considerable research studies which are looking from different control perspectives. Direct power control strategies which directly control stator power without rotor current control loops are reported in [9, 10]. Sliding mode controller structures [11, 12] are also important contributions which deal with energy maximization and robustness against disturbances. There are also reputable studies which consider robustness against grid voltage problems [13, 14, 15].

This study focuses on designing a novel robust stator voltage oriented DFIG controller structure with low pass filter first order disturbance observer. The main contribution of this paper is to achieve a simpler controller compared to basic conventional schemes given in [4, 5]. Machine dependent compensating terms are accurately estimated with the first order low pass filter disturbance observer. This prevents the necessity to accurately know the machine parameters which may deteriorate according to physical conditions. Decoupled proportional rotor current controllers are sufficient to separately control stator active and reactive power. The parameters of the actual 500KW DFIG in the MILRES (National Wind Energy Systems) project are used for the Matlab/Simulink based system model. The proposed current controller is also implemented on 1.1KW DFIG experimental test bed.

The rest of the paper is organized as follows. The dynamic equations of DFIG are given in chapter 2. Chapter 3 provides a controller structure based on a first order

disturbance observer. Simulation results of the proposed control structure are demonstrated in chapter 4. Experimental results are in chapter 5. Finally, 6th chapter gives the conclusion and proposes the future work.

2. DFIG Dynamic Equations

Before writing the dynamic equations L_r value could be written as follows.

$$L_r = L_{rb} + \Delta L_r \tag{1}$$

L_{rb} is the inductance value at fundamental frequency. ΔL_r is the value which is affected by frequency and other physical disturbances. DFIG dynamic equations in [1, 2] can be rewritten as follows;

$$V_s = L_s \frac{dI_s}{dt} + R_s I_s + L_m \frac{dI_r}{dt} + M_s(I_s + M_r I_r) \tag{2}$$

$$V_r = L_{rb} \frac{dI_r}{dt} + \Delta L_r \frac{dI_r}{dt} + R_r I_r + L_m \frac{dI_s}{dt} + N_s(I_r + N_r I_s) \tag{3}$$

The matrices V, I, M and N are defined as follows;

$$V = [v_d \quad v_q]^T \; I = [i_d \quad i_q]^T \tag{4}$$

$$M_s = \begin{bmatrix} 0 & L_s\omega_s \\ -L_s\omega_s & 0 \end{bmatrix}, \qquad M_r = \begin{bmatrix} 0 & \frac{L_m}{L_s} \\ -\frac{L_m}{L_s} & 0 \end{bmatrix} \tag{5}$$

$$N_s = \begin{bmatrix} 0 & L_s\omega_s \\ -L_s\omega_s & 0 \end{bmatrix}, \qquad N_r = \begin{bmatrix} 0 & \frac{L_m}{L_r} \\ -\frac{L_m}{L_r} & 0 \end{bmatrix} \tag{6}$$

All the rotor variables are referred to the stator side. The electromagnetic torque can be given as;

$$T_{em} = \frac{3}{2} p L_m (i_{rd} i_{sq} - i_{rq} i_{sd}) \tag{7}$$

Stator active and reactive Power equations can be written as;

$$P_s = \frac{3}{2}(v_{sd}i_{sd} + v_{sq}i_{sq}) \quad (8)$$

$$Q_s = \frac{3}{2}(v_{sq}v_{sd} - v_{sd}i_{sq}) \quad (9)$$

The equation of motion can be given as;

$$\frac{d\omega_m}{dt} = \frac{1}{J}(T_m - T_e + b.\omega_m) \quad (10)$$

3. Control System

3.1 Stator Voltage Angle Calculation

Rotating frames could be differently aligned in the literature. Stator voltage angle is aligned with d axis, with $v_s=v_{sd}$ and $v_{sq}=0$. The voltage vectors and reference frames are in figure 1.

The voltage angle could be calculated by using,

$$\theta_s = \arctan(\frac{v_{s\beta}}{v_{s\alpha}}) \quad (11)$$

However, phase lock loop (PLL) techniques which are more robust against voltage disturbances are widely used for phase and frequency detection of the voltage signal. Different PLL techniques could be encountered in the literature [16]. A basic PLL algorithm which is given in figure 2 is used in simulations and experiments of this study. Grid voltages, transformed into dq coordinate system are the inputs of the algorithm. Q component of the voltage could be forced to be zero with a PI controller. Output of the PI controller is the grid frequency. Integration of the grid frequency is the position of the signal. This position is used in the abc-dq calculation.

3.2 Design of Current Controllers

DFIG rotor voltage equation in (3) must be rewritten to simply design proportional rotor current controllers. All currents and voltages could be measured in real applications without any problems. However, machine parameters may deteriorate according to physical conditions. The aim of rewriting the equations is to separate the machine dependent and independent terms. Therefore, a simpler controller structure could be achieved. Rotor dynamics in (3) could be rewritten as follows;

$$\frac{dI_r}{dt} = \frac{V_r}{L_{rb}} + (\underbrace{-\frac{R_r}{L_r}V_r - \frac{L_m}{L_r}\frac{dI_s}{dt} + N_s(I_s + N_r I_r) - \Delta L_r \frac{dI_r}{dt}}_{\hat{V}_r^{dis}}) \quad (12)$$

The vector V_r^{dis} is defined as $V_r^{dis} = \begin{bmatrix} v_{rd}^{dis} & v_{rq}^{dis} \end{bmatrix}$ that is considered as parameter dependent disturbance terms. Equation (12) could be simplified as follows.

$$\frac{dI_r}{dt} = \frac{V_r}{L_{rb}} + V_r^{dis} \quad (13)$$

Derivative of errors for rotor currents can be written as;

$$\frac{d\varepsilon_r}{dt} = \frac{dI_r^{ref}}{dt} - \frac{dI_r}{dt} \quad (14)$$

Where $\varepsilon_{rd} = [\varepsilon_{rd} \quad \varepsilon_{rq}]^T$

(13) and (14) could be written with (14) as follows;

$$\frac{d\varepsilon_r}{dt} = -\frac{V_r}{L_{rb}} - (-\frac{dI_r^{ref}}{dt} + V_r^{dis}) \quad (15)$$

Next, the desired closed loop dynamics can be written as;

$$\frac{d\varepsilon_r}{dt} + K\varepsilon_r = 0 \quad (16)$$

Where $K = [k_d \quad k_q]$ is defined as proportional controller gain.

If (15) is written to (16) desired closed loop dynamics is rewritten as follows;

$$-\frac{V_r}{L_{rb}} + \left(\frac{dI_r^{ref}}{dt} + V_r^{dis}\right) - K\varepsilon_r = 0 \quad (17)$$

Rotor voltage equations could be obtained by rewriting (17)

$$V_r^{ref} = L_{rb}\left(\frac{dI_r^{ref}}{dt} + V_r^{dis} + K\varepsilon_r\right) \quad (18)$$

If the effect of $\frac{dI_r^{ref}}{dt}$ is neglected, control effort could be expressed as follows.

$$V_r^{ref} = V_r^{dis} + L_{rb}K\varepsilon_r \quad (19)$$

3.3 Disturbance Observer

In this section, the derivation of the disturbance observer is presented. The vector V_r^{dis} is the disturbance term which is dependent on physical conditions. Controller structure could be finalized, if the disturbances are correctly estimated.

$$V_r^{dis} = V_r - L_{rb}\frac{dI_r}{dt} \quad (20)$$

Writing (22) in s domain and implementing first order low pass filter disturbance observer concept [17];

$$\hat{V}_r^{dis} = \left(V_r - L_{rb}\frac{dI_r}{dt}\right)\frac{g}{s+g} \quad (21)$$

The estimation error can be expressed as;

$$V_r^{dis} - \hat{V}_r^{dis} = \left(V_r - L_{rb}\frac{dI_r}{dt}\right) - \left(V_r - L_{rb}\frac{dI_r}{dt}\right)\frac{g}{s+g} = \left(1 - \frac{g}{s+g}\right)V_r^{dis} \quad (22)$$

The estimation error converges to zero. The vector $\hat{V}_r^{dis} = \begin{bmatrix}\hat{v}_{rd}^{dis} & \hat{v}_{rq}^{dis}\end{bmatrix}$ is parameter dependent estimated disturbance. The term g is the cut-off frequency of the low pass filter in radians. It is obvious from (21) that $\hat{v}_{rd}^{dis}$ and $\hat{v}_{rq}^{dis}$ are independent from machine parameters. As a result, block diagram in figure 3 can be obtained. Decoupled control of active and reactive power could be achieved by controlling i_{rq} and i_{rd}

respectively. This control structure can be implemented in speed, torque or power control of DFIG. Maximum power point tracking (MPPT) algorithms can be followed according to any wind turbine dynamics.

4. Simulation Results

More accurate simulation platform is obtained compared to [3] without necessity of reduced order models by using discretized model of DFIG. 100μs sample time in Matlab/Simulink is used in simulations. Inverter dynamics are neglected. 500KW DFIG parameters [18] which will be used in MILRES project is given in Table 1. All the rotor parameters are referred to the stator side. Control system can work in different scenarios. In this study, generator is controlled according to speed control strategy.

Machine parameters dependent compensating terms of control structure is estimated by disturbance observer. Basically, two different step response tests are applied in one simulation at different time instants. Speed reference is changed from 60 to 90 rad/s (from sub synchronous to super synchronous speed) at 10^{th} second. Wind torque reference is changed from 3000Nm to 5000Nm at 12^{th} second. It is expected that system must follow the speed (Figure 4) and wind torque (Figure 5), while accurately estimating disturbance terms. There is a huge current torque and current increase at 10^{th} second of simulation. The reason of high current and torque is the speed step which is deliberately applied with a high speed controller gain in order to check the performance of the controller structure. Control system could handle this dramatic step and kept stable. i_{rd} reference (Figure 6) is kept zero during the simulations.

It is obviously seen from the simulation results that DFIG dynamic model works properly and compensating terms are accurately estimated by disturbance observer (Fig. 9-10). Rotor power is changing the direction while the speed changes from subsynchronous to supersynchronous speed (Figure 8). Active and reactive stator powers are decoupled (Figure 7). Performance of the speed controller could be modified (Figure 4) according to physical conditions. However, focus of the simulation results is accurately estimating compensating terms.

5. Experimental Results

Experimental setup in Figure 11 is used in the experiments. A squirrel cage induction machine (SCIM) driven by a commercial inverter which represents the wind. DFIG plate data is given in Table 2. Controller algorithm is generated in dSPACE DS1103 by using Controldesk C language. Sample time of the control structure is 100μs. Semikron Semistack (21f_b6u_e1cif_b6ci_12_v12) inverter used in experiments and 120VDC constant voltage power is directly applied to DC link. Switching frequency is 10 kHz. Low pass filter cut-off frequency (g) is chosen as 1200. Proportional gains of the controllers (k_p and k_q) are 100. These values are found in trial and error method in the experiments without any algebraic calculations.

5.1 Experiment 1

The aim of the first experiments is to show that decoupled control of I_{rd} and I_{rq} rotor currents separately changes the stator active and reactive power respectively. DFIG is rotated in constant subsynchronous speed by SCIM. I_{rd} and i_{rq} step response tests are

applied in different experiments, and the change of stator reactive and active power is demonstrated respectively.

It is obvious from the experimental results that both rotor current controllers accurately change stator active and reactive power (Figure 13 and 16). Compensating terms also change (Figures 14 and 17)when step responses are applied.

5.2 Experiment 2

The main objective of DFIG based wind turbines is decoupled control of active and reactive power. Control structure given in figure 3 is implemented by using basic PI power controllers in the outer loop while generator is driven by SCIM at arbitrary speed. Active and reactive power step response tests are applied and decoupled control of active and reactive stator power could be achieved.

Conclusion

Decoupled control of active and reactive power with a first order low pass filter disturbance observer is fully demonstrated with the simulation and experimental results. It is shown that compensating terms are accurately estimated by the disturbance observer in simulations. Experimental results validate the accuracy of the proposed control method by effectively achieving stator active and reactive power flow.

References

[1] Montenau I, Bratcu AI, Cutululis NA, Ceanga E. Optimal Control of Wind Energy Systems: Towards a Global Approach. Advances in Industrial Control: Springer, 2008.

[2] Leonard W. Control of electric drives. 3rd Edition. Berlin, Heidelberg, Springer: New-York, 2003.

[3] Akhmatov V. Analysis of dynamic behavior of electric power systems with large amount of wind power. PhD thesis, Technical University of Denmark, April 2003.

[4] Pena R, Clare JC, Asher GM. A doubly-fed induction generator using two back-to-back PWM converters and its application to variable speed wind energy system. Proc. IEE, 1996; vol. 143, pp.231–241.

[5] Muller S, Deicke M, and De Doncker RW. Doubly fed induction generator systems for wind turbines, IEEE Ind. Appl. Mag. May/Jun. 2002, vol. 8, pp. 26–33.

[6] Li S, Challoo R, Nemmers MJ. Comparative study of DFIG power control using stator-voltage and stator-flux oriented frames. Power&Energy Society General Meeting, 2009; Canada: IEEE, pp. 1-8.

[7] Demirok E. Grid-connected variable speed generator applications with doubly-fed induction machine, Msc. thesis , Sabancı University, Summer 2007.

[8] Tapia G, Santamaria G, Telleria M, Susperregui A. Methodology for smooth connection of doubly fed induction generators to the grid. IEEE Trans. on Energy Conversion, Dec. 2009; Vol. 24 pp. 959-971.

[9] Xu L, Cartwright, P. Direct active and reactive power control of DFIG for wind energy generation. IEEE Transactions on Energy Conversion, 2006, Vol. 3, pp. 750-758.

[10] Zhi D, Xu L. Direct power control of DFIG with constant switching frequency and improved transient performance. IEEE Trans. on Energy Conversion, March 2007; Vol.22, pp.110-118.

[11] Battista HD, Mantz RJ. Dynamical variable structure controller for power regulation of wind energy conversion systems, IEEE Trans. On Energy Conversion, 2004; Vol.4, pp.756-763.

[12] Beltran B, BenBouzid MEH, Ahmet-Ali T. High order sliding mode control of a DFIG based wind turbine for power maximization and grid fault tolerance. Electric Machines and Drives Conference (IEMDC), 2009; USA: IEEE, pp 183-189.

[13] Luna A, Rolan A, Medeiros G, Rodrigez P, Teodorescu R. Control strategies for DFIG wind Turbines Under Grid Fault Conditions, 35th Annual Conference of IEEE Industrial Electronics, (IECON) 2009; Portugal pp 3886-3891.

[14] Rodriguez P, Luna A, Teodorescu R, Iov F, Blaabjerg F, Fault ride-through capability implementation in wind turbine converters using a decoupled double synchronous reference frame PLL, European Conference on Power Electronics, 2007; Denmark: pp. 1–10.

[15] Zhou P, Yikang H, Sun D. Improved direct power control of a DFIG-Based wind turbine during network unbalance. IEEE Transactions on Power Electronics, 2009; Vol. 11, pp. 2465-2474.

[16] Blaabjerg F, Teodorescu R, Liserre M, Timbus AV. Overview of control and grid synchronization for distributed power generation systems, IEEE Transactions on Industrial Electronics, 2006 Vol. 5, pp. 1398-1409.

[17] Ohnishi K, Shibata M, Murakami T, Motion control for advanced mechatronics, IEEE/ASME Transactions on Mechatronics, March 1996 Vol.1, pp 56–67.

[18] TUBITAK Report. Generatör Elektriksel ve Manyetik Analiz Detay Tasarım Raporu (DFIG), R-1.1.1", June 2013.

FIGURES

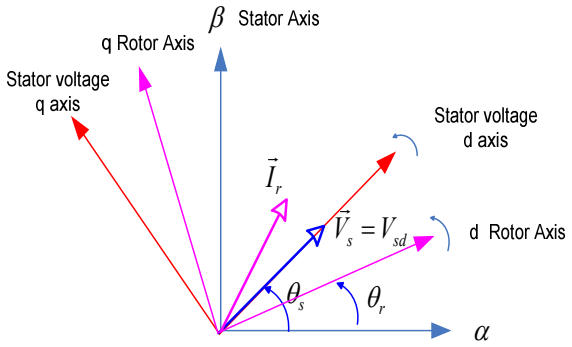

Figure 1. Voltage Vectors and Reference Frames

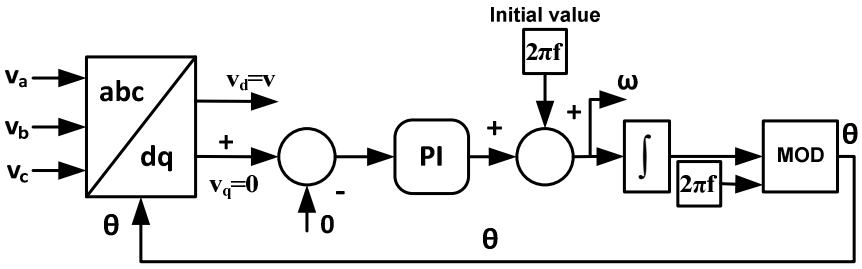

Figure 2. PLL algorithm

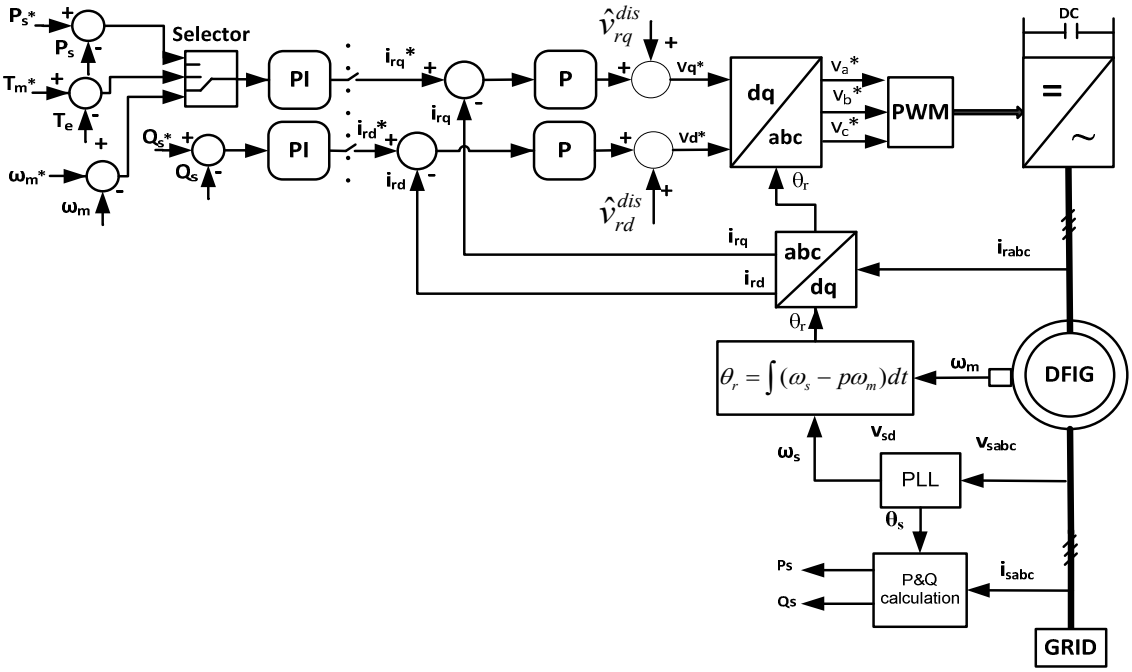

Figure 3. Proposed Control Diagram

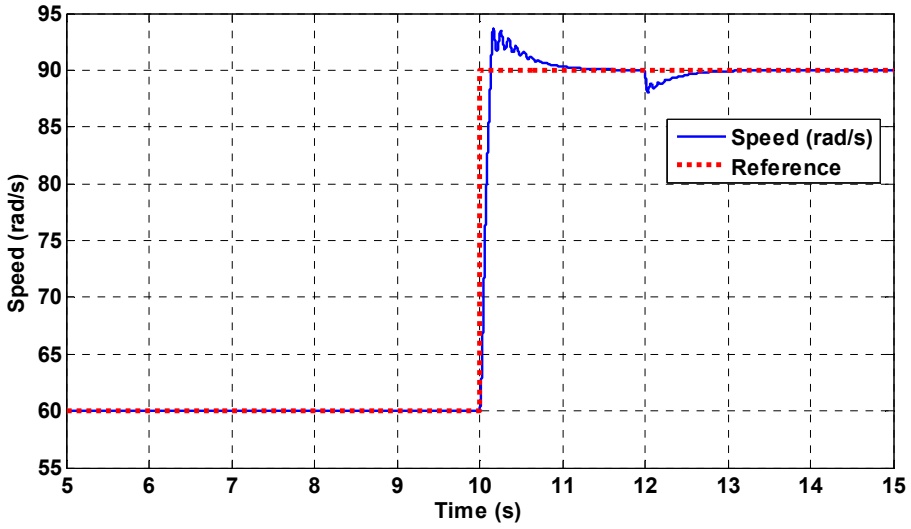

Figure 4. Actual and Reference Speed

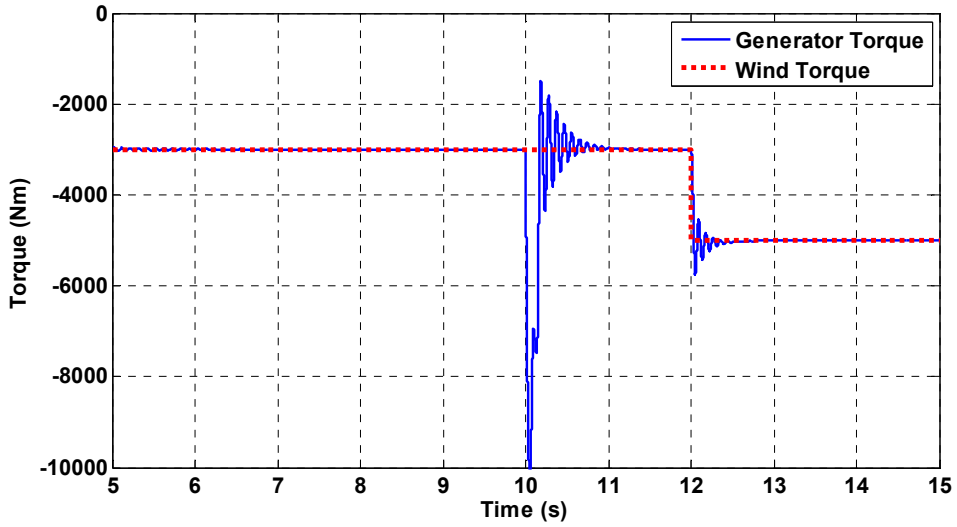

Figure 5. Generator Torque & Wind Torque

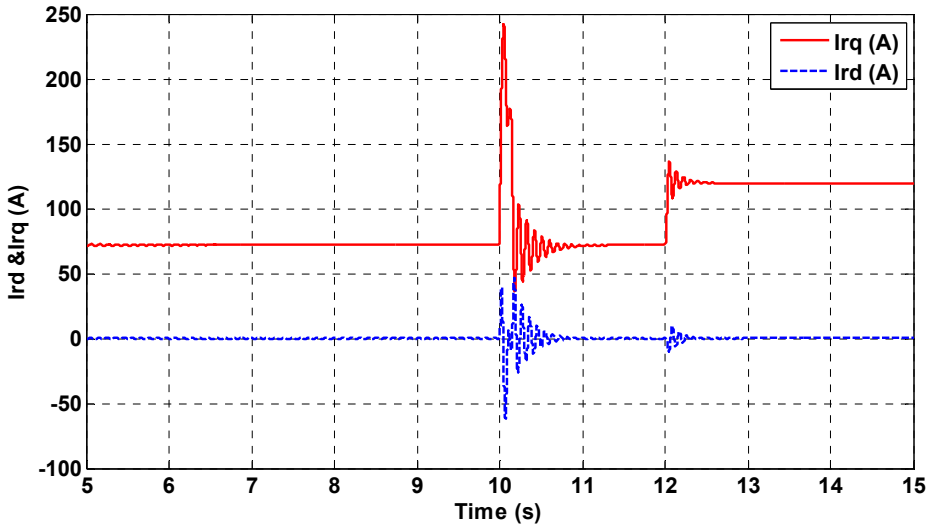

Figure 6. Rotor currents

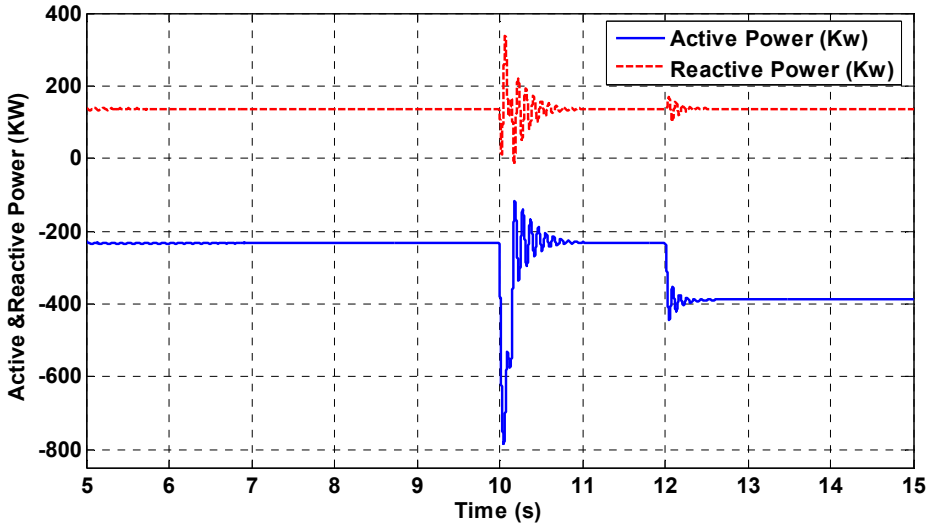

Figure 7. Stator Active & Reactive Power

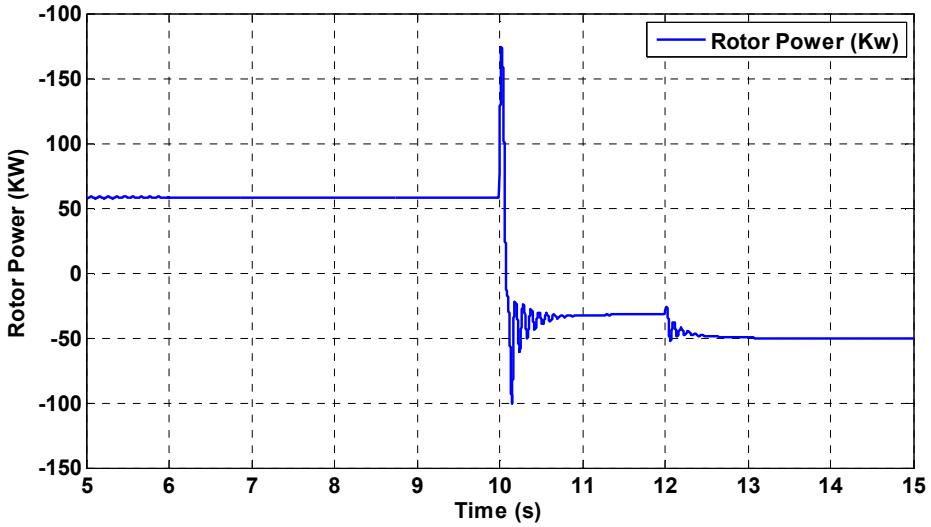

Figure 8. Rotor Active Power

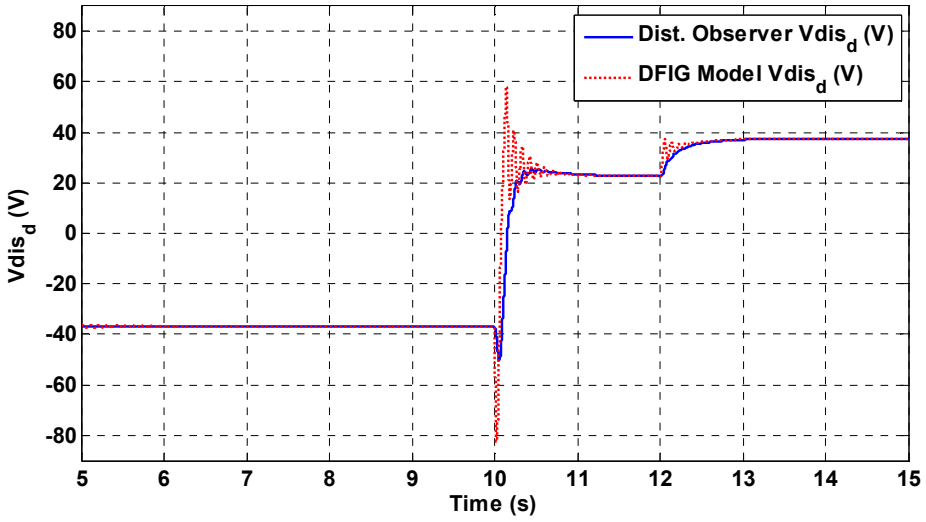

Figure 9. Estimated & Modeled Disturbance Terms (v_{disd})

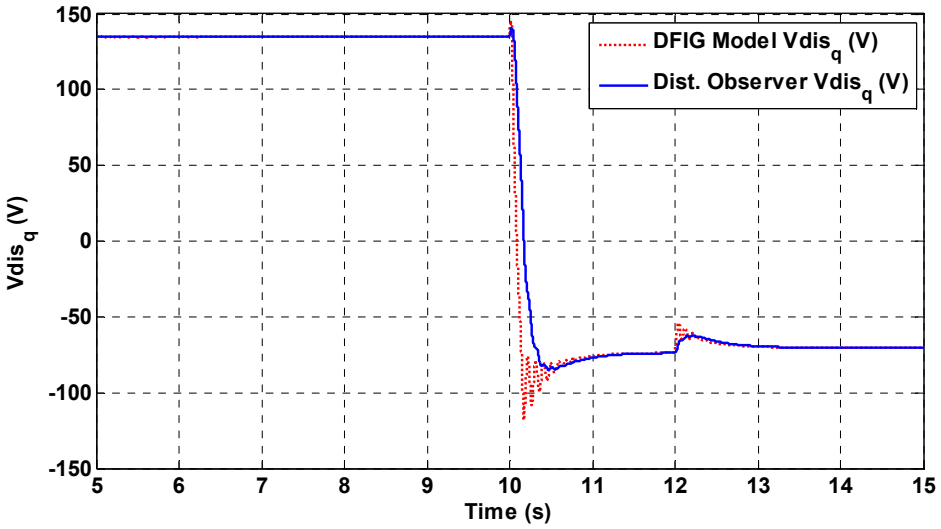

Figure 10. Estimated & Modeled Disturbance Terms (v_{disq})

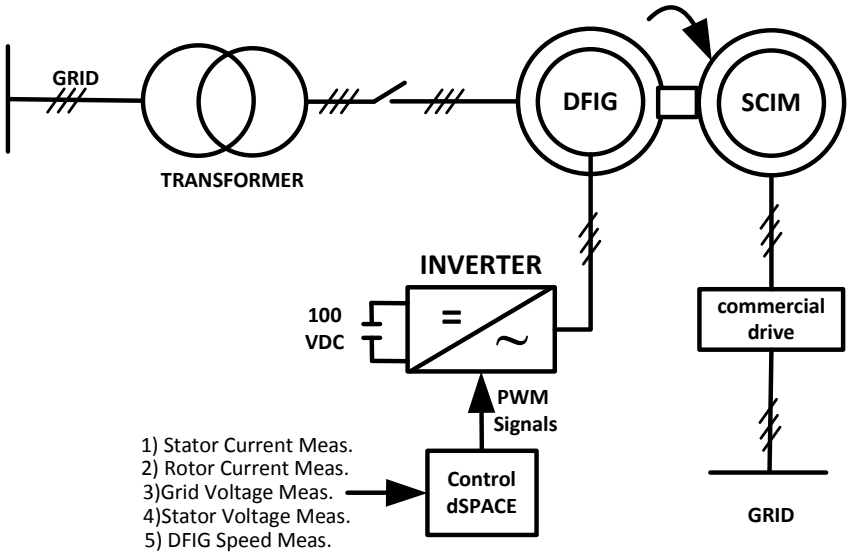

Figure 11. Experimental Set up

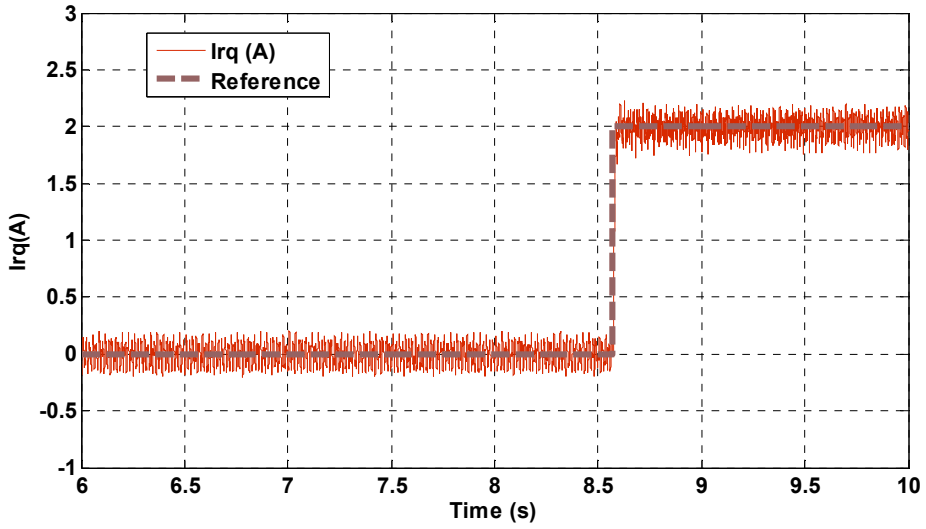

Figure 12. Experiment 1-A I_{rq} step response

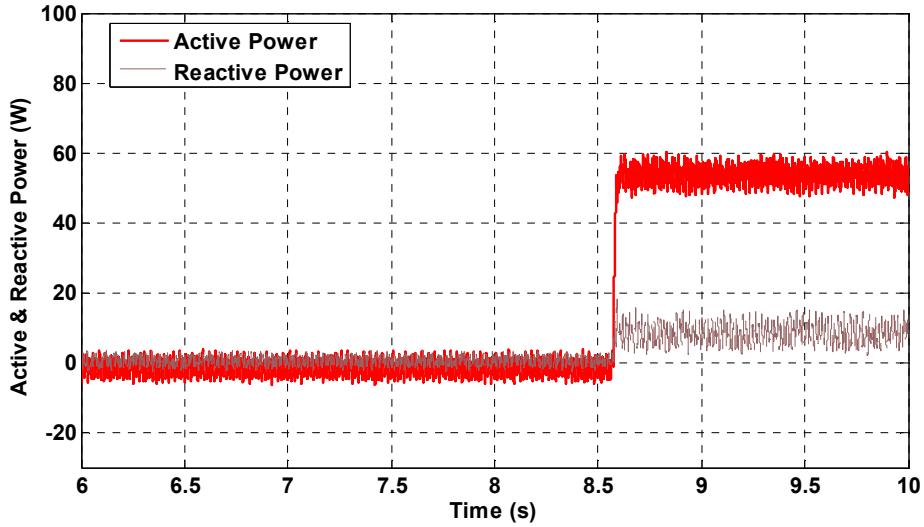

Figure 13. Experiment 1-A Change of Active & Reactive Power

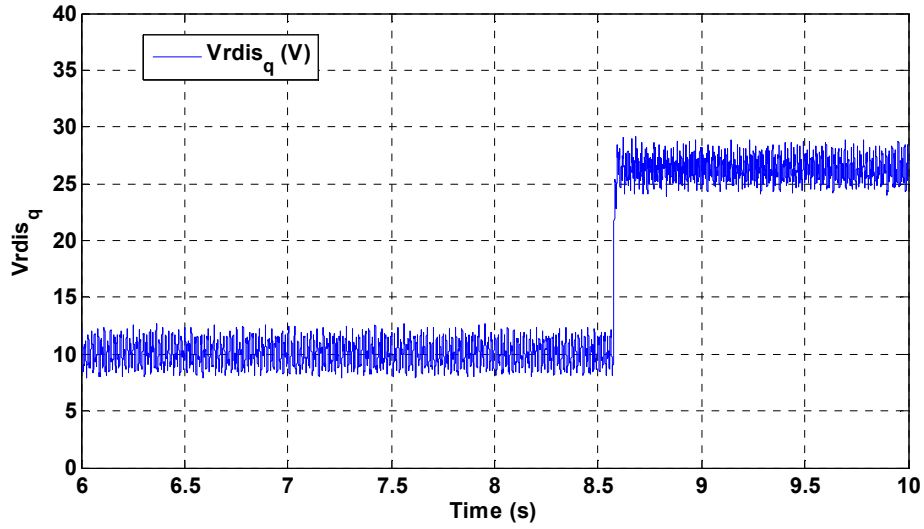

Figure 14. Experiment 1-A Compensating Term Sq

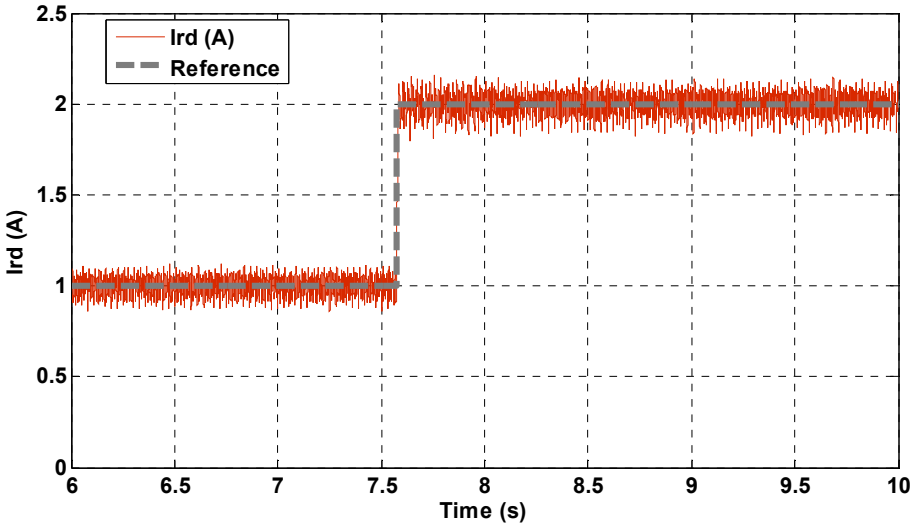

Figure 15. Experiment 1-B I_{rd} step response

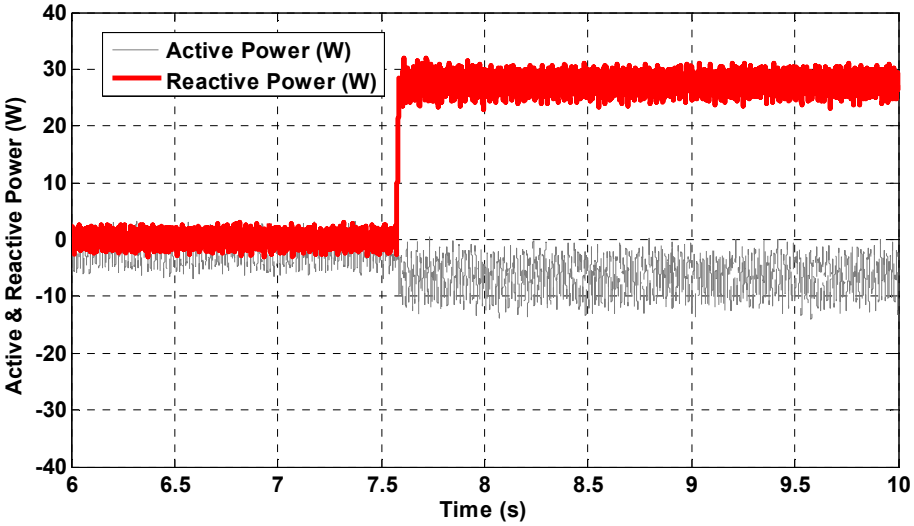

Figure 16. Experiment 1-B Change of Active & Reactive Power

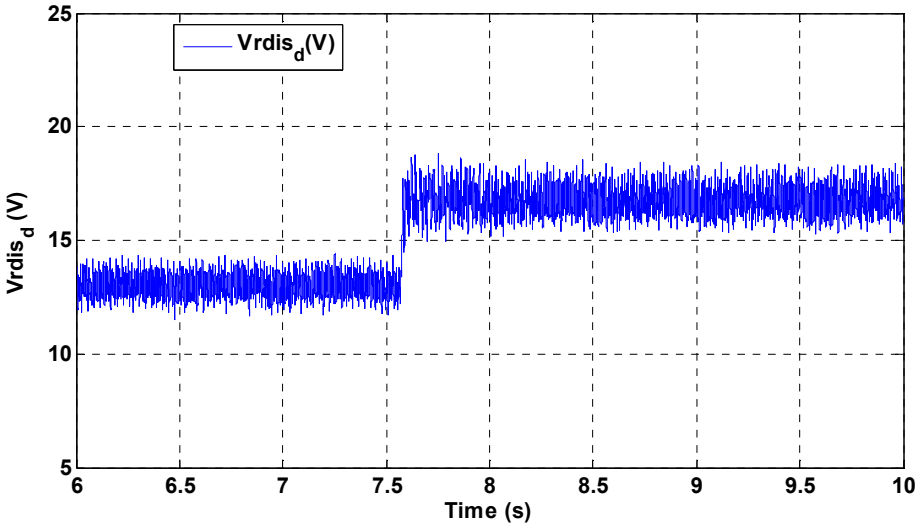

Figure 17. Experiment 1-B Vrdis_d

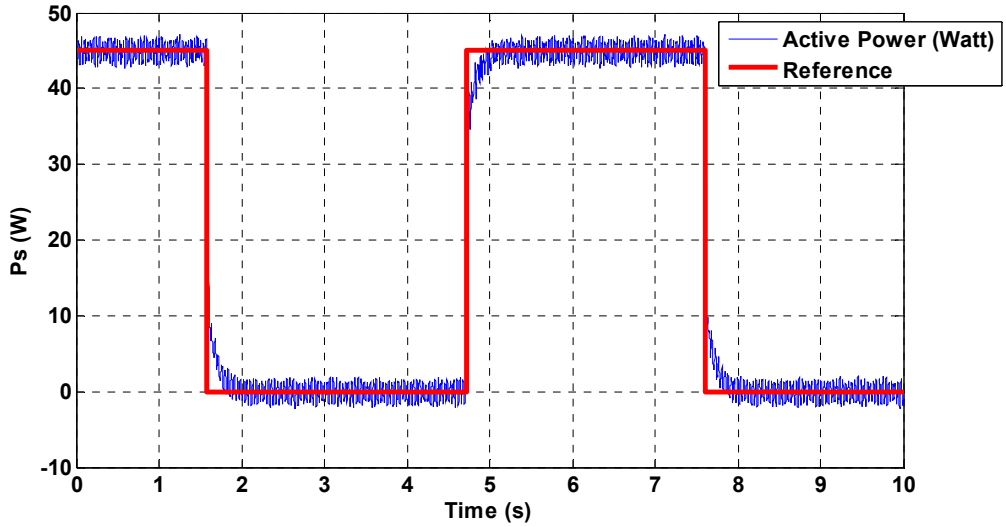

Figure 18. Experiment 2-A Active Power Response Test

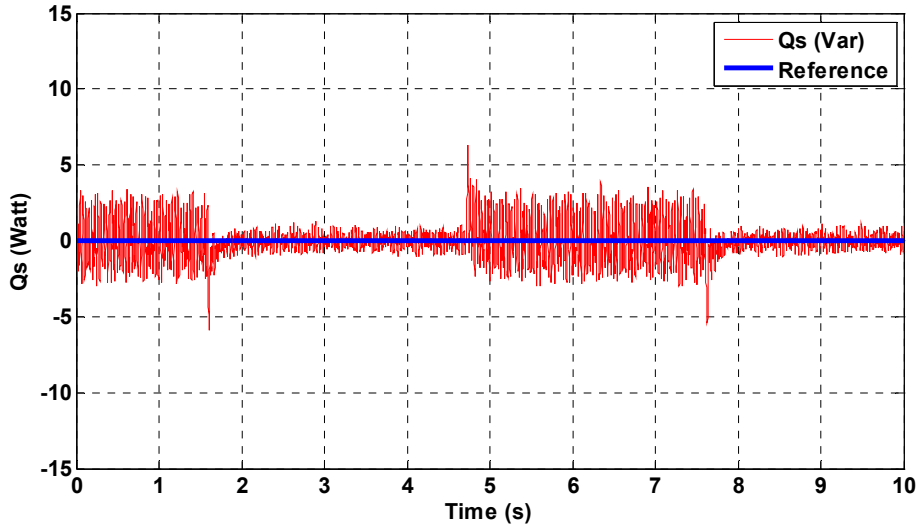

Figure 19. Experiment 2-A Reactive Power at Active Power Step Response Test

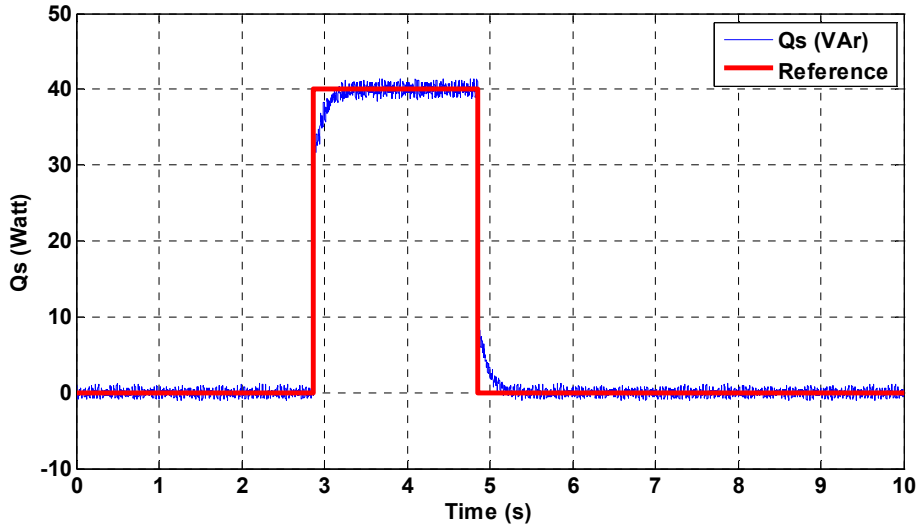

Figure 20. Experiment 2-B Reactive Power Response Test

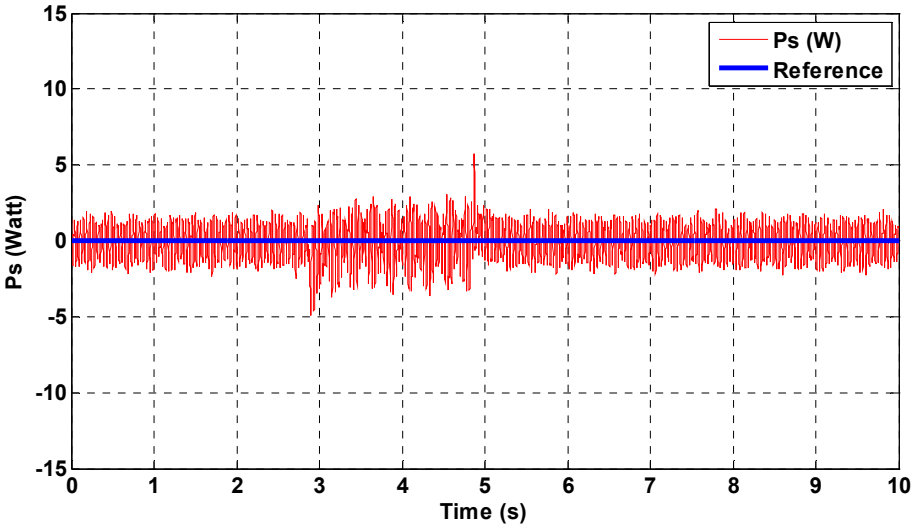

Figure 21. Experiment 2-B Active Power at Reactive Power Response Test

TABLES

Table 1. DFIG parameters in simulation

Stator Power (P_s)	457.6	KW
Rotor Power (P_r)	61.4	KW
Stator Voltage	690	V
Number of Poles (p)	4	
Slip Variation	0.25	
Nominal Torque	6784	Nm
Synchronous Speed	750	rpm
Stator Resistance (R_s)	0,018	ohm
Rotor Resistance (R_r)	0,021	ohm
Mutual Inductance (L_m)	0,011	H
Stator Inductance (L_s)	0,012	H
Rotor Inductance (L_r)	0,012	H
Turn Ratio (n_s/n_r)	4	
Moment of Inertia	22	kgm^2

Table 2. DFIG plate data in experiments

Power	1,1	KW
Stator Voltage	220/380	V (D/Y)
Stator Current	6,4/3,7	A
Power Factor	0,67	
Speed	1360	rpm
Rotor Voltage	70	V
Rotor Current	12	A